

Error Analysis for Image Inpainting ^{*}

Tony F. Chan [†] and Sung Ha Kang [‡]

Abstract

Image inpainting refers to restoring a damaged image with missing information. In recent years, there have been many developments on computational approaches to image inpainting problem [2, 4, 6, 9, 11, 12, 13, 27, 28]. While there are many effective algorithms available, there is still a lack of theoretical understanding on under what conditions these algorithms work well. In this paper, we take a step in this direction. We investigate an error bound for inpainting methods, by considering different image spaces such as smooth images, piecewise constant images and a particular kind of piecewise continuous images. Numerical results are presented to validate the theoretical error bounds.

Key words: Inpainting, Total Variation minimization, error analysis, inpainting domain, image restoration

1 Introduction

Image inpainting refers to a specific image restoration task, where missing or damaged portions of an image are reconstructed. For example, cracks on old oil paintings or letters covering parts of magazine photos would be considered the missing or damaged portions of an image. Inpainting methods use the known image information to recover those missing areas.

Masnou and Morel [28] addressed this as a disocclusion problem, and used an explicit geometric level line interpolation procedure to recover the occluded regions. Bertalmio et al. [4] first introduced the notion of digital image inpainting and use third order partial differential equations (PDE) to diffuse the known image information into the missing regions along the level lines. Later, this inpainting approach was extended to include the direction of the level lines [2] and related to the Navier-Stokes equation [3]. An alternative variational approach was proposed by Chan and Shen [11] that minimizes the total variation of recovered image while fitting the known information (TV inpainting). This method is later extended by adding the Euler's Elastica to the variational functional in [9] in order to allow the curved level lines to be recovered. We follow these variational approaches in this paper. Some methods are more efficient in computation than others while producing similar results (unless higher order method is used) and, since variational models are best suited for error analysis, we consider harmonic and TV inpainting models in this paper. Many inpainting methods have proved very successful, and been addressed in several recent articles [16, 30, 31, 32]. Further studies include texture inpainting [5], and Wavelet inpainting [15] and inpainting from multiple view [25, 26]. More related literature can be found in [6, 12, 13, 14, 27, 33].

In general, image inpainting can be described as follows. Let Ω be the image domain, $u_o : \Omega \rightarrow \mathbb{R}_+ \cup \{0\}$ be the given original image, and domain $D \subset \Omega$ represents the region with missing information. We refer to domain D as the *inpainting domain*, and we assume it has already been identified. This D is a closed set with smooth continuous boundary, and ∂D denotes the inpainting boundary $\partial D \in \Omega \setminus D$. Variational image inpainting methods use information from outside the inpainting domain by minimizing a regularization

^{*}We acknowledge supported by grants from the NSF under contracts DMS-0312223, DMS-9973341, ACI-0072112, INT-0072863, the ONR under contract N00014-03-1-0888, the NIH under contract P20 MH65166, and the NIH Roadmap Initiative for Bioinformatics and Computational Biology U54 RR021813 funded by the NCCR, NCBC, and NIGMS.

[†]Department of Mathematics, UCLA, Los Angeles, CA 90095-1555, USA, (chan@math.ucla.edu),

[‡]Department of Mathematics, University of Kentucky, Lexington, KY 40515, USA, (skang@ms.uky.edu)



Figure 1: (a) and (b) are the same image with two different inpainting domains. Both inpainting domains have the same total area, yet inpainted result (a) looks better than inpainted result of (b).

functional such as,

$$\min \mathcal{E}(u) = \min \int_D g(u) dz \quad \text{s.t.} \quad u = u_o|_{\partial D}. \quad (1)$$

We consider two functions for g in this paper; one is $g(u) = |\nabla u|^2$, which we refer to as *harmonic inpainting*, and the other is $g(u) = |\nabla u|$, which is the TV inpainting [11]. For general images, harmonic inpainting is not appropriate since it tends to smooth out the edges. However, we consider it in this paper, since harmonic inpainting is more natural for inpainting smooth images, and the error term can be carried out more theoretically. We consider harmonic inpainting for smooth images, and TV inpainting for images with discontinuities.

In this paper, we are interested in the error bound for such inpainting problems. Intuitively, if more pixels are missing, one can expect to have a bigger error. However, the purpose of this error analysis is to show that the error depends more on the geometry and the shape of the inpainting domain than the size or total area of the inpainting domain. For example, in Fig. 1, two image (a) and (b) have two different inpainting domains with exactly the same total area; however, the inpainted image (a) looks much better

than the inpainted image (b). The inpainting results are dependent on the shape of the inpainting domain, and most of the local inpainting methods are known to work well with “narrow” inpainting domains. One of the purpose of our paper is to understand this phenomenon.

The outline of this paper is as follows. In Section 2, we consider smooth functions with harmonic inpainting, and use Green’s function representation to analyze the error. Preliminary work has been done by Chan and Shen [11], and the outline of their study as well as more refined results are covered in the section. In Section 3, we consider piecewise constant images with TV inpainting, and use a level line analysis to consider a region where the error may occur. For the piecewise constant case, the error is dependent on the geometric details of how the level lines meet with the boundary of the inpainting domain. In Section 4, we study a particular type of piecewise continuous functions with TV inpainting by utilizing results from the previous sections. We present numerical experiments in Section 5 to illustrate the aspects of the theory, which is followed by concluding remarks in Section 6.

2 Harmonic Inpainting for Smooth Functions

In 1-dimension, the inpainting domain D is an interval, and inpainting problem can be seen as an interpolation of the two end-points of interval D . The error term for such interpolation is bounded by the smoothness of the function and the length between the two end-points. This is also true in the 2-dimensional case. We consider inpainting as an interpolation of the boundary information such as in equation (1), and define the error as

$$err(z) = |u(z) - u_{true}(z)|, \quad \text{for } \forall z \in D. \quad (2)$$

Here, u_{true} is the *true image* without any inpainting domains, u_o is the given *original image* with an inpainting domain D , and u is the interpolation. In this section, we assume u, u_o , and u_{true} are all smooth functions: $u, u_o, u_{true} \in C^2(\Omega)$. Note that the error, $err(z)$, is a point-wise error, and the total error over D is

$$err(D) = \int_D err(z) dz \leq |D| \max_{z \in D} \{err(z)\}.$$

where $|D|$ is the area of the inpainting domain.

For a smooth function, one natural choice for an interpolation is a harmonic extension. Therefore, by considering the solution of the Laplace’s equation, we can express the error, $err(z)$, using Green’s function. Assuming D has a smooth boundary, the energy functional for harmonic inpainting is

$$\min \int_D |\nabla u|^2 dz \quad \text{s.t.} \quad u = u_o|_{\partial D}. \quad (3)$$

The Euler-Lagrange equation of this functional is equivalent to solving the Laplace’s equation: $\Delta u = 0$, $z \in D$ and $u = u_o$, $z \in \partial D$. As in PDE references [17, 19, 23], if there is a Green’s function G for this domain D , then the solution of (3) is

$$u(z_o) = - \int_{\partial D} u_o(z(s)) \frac{\partial(G(z_o, z))}{\partial \eta} ds, \quad (4)$$

where η is the outward normal direction along ∂D , s is the arc-length parameter of ∂D , and $G(z_o, z)$ is the Green’s function satisfying $-\Delta G = \delta(z - z_o)$ for $z_o \in D$ and $G|_{\partial D} = 0$ on ∂D . On the other hand, the true image u_{true} satisfies: $-\Delta u_{true} = f$ for $z \in D$, and $u_{true} = u_o$ for $z \in \partial D$ (where $f = -\Delta u_{true}$ by definition). Thus, this u_{true} can be expressed as

$$u_{true}(z_o) = - \int_{\partial D} u_o(z(s)) \frac{\partial(G(z_o, z))}{\partial \eta} ds + \int_D f(z) G(z_o, z) dz.$$

Here, the first term is the interpolation solution to the harmonic inpainting (4). The second term is the anti-harmonic term, which gives the error term in (2). Since we assume the image is smooth, we can define

the bound for the smoothness to be M , such that $|\Delta u| \leq M$ in D . Therefore, for each $z_o \in D$, the error is bounded by

$$err(z_o) = \left| \int_D f(z)G(z_o, z)dz \right| \leq M \int_D G(z_o, z)dz. \quad (5)$$

This is the harmonic inpainting error bound for a smooth function, and we focus on this integral of a Green's function throughout this section.

2.1 Review of Green's function approach

This section is an outline of lemmas and theorem given in [11], some of which are needed to refine the error bound.

Lemma 1 (*Comparison Lemma*) Suppose two domains, D_1 and D_2 , and their corresponding Green's functions, $G_1(z_o, z)$ and $G_2(z_o, z)$, are defined. If $D_1 \subset D_2$, then $\forall z_o, z \in D_1$,

$$G_1(z_o, z) \leq G_2(z_o, z).$$

Lemma 2 Suppose B_1 is a unit disk centered at 0, and $G_1(z_o, z)$ is its corresponding Green's function. Then, for all $z_o \in B_1$,

$$\int_{B_1} G_1(z_o, z)dxdy = \frac{1 - |z_o|^2}{4}.$$

Theorem 1 Let d denote the diameter of a domain D and $G(z_o, z)$ be the associated Green's function for the Poisson equation on D . Then

$$\int_D G(z_o, z)dxdy \leq \frac{d^2}{4}.$$

Theorem 1 is proved in [11] by covering the inpainting domain D with a disk B_1 with a diameter d , and by using Lemma 1 to show that the integral of the Green's function over D is smaller than that over B_1 . Using the bound M for the smoothness and Lemma 2, the error for $\forall z_o \in D$ was bounded by,

$$err(z_o) \leq M \int_D G(z_o, z)dz \leq \frac{Md^2}{4}. \quad (6)$$

This result says, for any point z_o inside D , the point-wise intensity error, $err(z_o)$, is bounded by a term proportional to the square of the radius of a disk covering D .

2.2 Long and narrow inpainting domains

The bound (6) is somewhat pessimistic if the shape of the inpainting domain D is not close to a circle. In particular, if D is a long and narrow domain, the bound (6) doesn't give an insight on the error. For example, Fig. 2 shows a smooth function with harmonic inpainting with two different shapes of the inpainting domain D_1 and D_2 . Image (a) requires a bigger diameter disk covering D_1 ; however, the inpainted image (a) looks better than the inpainted image (b). In a real experiment, the inpainted result depends more on the "width" of the inpainting domain than the radius of the disk covering the inpainting domain. Therefore, for a long and narrow region, one can expect to refine the error bound. In the following Lemma, we use an ellipse to cover the inpainting domain and refine the error bound from (6).

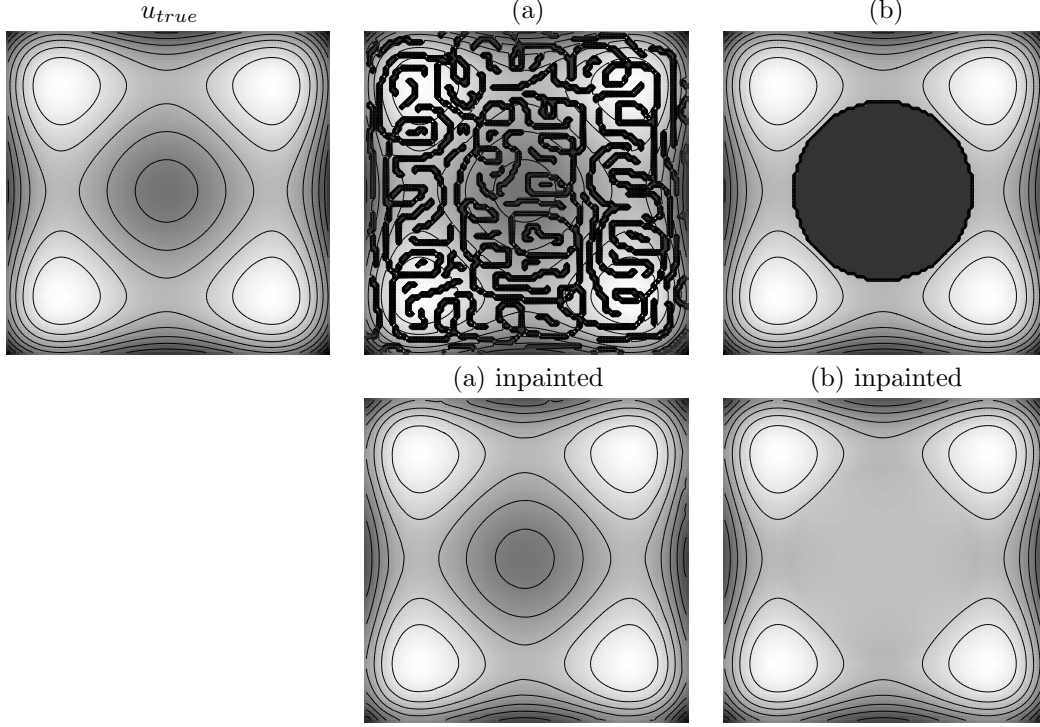


Figure 2: Harmonic inpainting for a smooth function. All images are superposed with each contour plots. (a) u_o with inpainting domain D_1 , and (b) u_o with a different circle-shaped inpainting domain D_2 . Image (a) has a bigger diameter disk covering D_1 than that covering D_2 ; however, (a) inpainted is closer to u_{true} compared to (b) inpainted. D_1 and D_2 have the same total area.

Lemma 3 Suppose $B_e(\alpha/2, \beta/2)$ is an ellipse centered at 0, $\frac{x^2}{(\alpha/2)^2} + \frac{y^2}{(\beta/2)^2} = 1$, where $\alpha \geq \beta$, and $G_2(z_o, z)$ it's Green's function. Then, for $z_o = (x_o, y_o) \in B_e$,

$$\int_{B_e} G_2(z_o, z) dx dy \leq \frac{\beta^2}{8}.$$

Proof. Consider the following Poisson equation on ellipse $B_e(\alpha/2, \beta/2)$,

$$-\Delta v = 1, \quad v|_{\partial B_e} = 0.$$

Then the unique solution v becomes,

$$v(z) = \frac{1 - \frac{x^2}{(\alpha/2)^2} - \frac{y^2}{(\beta/2)^2}}{\frac{2}{(\alpha/2)^2} + \frac{2}{(\beta/2)^2}} \left(= \frac{\frac{\beta^2}{4} - \frac{\beta^2}{\alpha^2}x^2 - y^2}{2\frac{\beta^2}{\alpha^2} + 2} \right).$$

On the other hand, using the Green's function, $v(z_o)$ can also be expressed as

$$v(z_o) = \int_{B_e} G_2(z_o, z) (-\Delta u(z)) dx dy = \int_{B_e} G_2(z_o, z) dx dy.$$

Therefore, the bound for the Green function on the ellipse B_e becomes,

$$\int_{B_e} G_2(z_o, z) dx dy = \frac{\frac{\beta^2}{4} - \frac{\beta^2}{\alpha^2}x_o^2 - y_o^2}{2\frac{\beta^2}{\alpha^2} + 2} \leq \frac{\beta^2 - 4y_o^2}{8}.$$

For any point $z \in B_e$, the integral of Green's function is bounded by $\frac{\beta^2}{8}$, since $-\frac{\beta}{2} \leq y_o \leq \frac{\beta}{2}$. \square

This Lemma shows that the integral of Green's function for an ellipse is bounded by $\frac{\beta^2}{8}$. We define β to be a *minor diameter* of the ellipse (and α to be the *major diameter* of the ellipse). Using the error bound (5), error term for harmonic inpainting is bounded by a term proportional to the square of the minor diameter of the ellipse covering D .

Theorem 2 For any point in the inpainting domain, $z_o = (x_o, y_o) \in D$, the point-wise intensity error, $err(z_o) = |u(z_o) - u_{true}(z_o)|$, is bounded by

$$err(z_o) \leq \frac{M}{8}\beta^2, \quad (7)$$

where M is a bound for the smoothness of u , $|\Delta u(z)| \leq M$, and β is the minor diameter of an ellipse covering the inpainting domain D .

Proof. For a given inpainting domain, let B_e be an ellipse covering D . For simplicity, translate and rotate D and B_e that the center of B_e is on the origin, and the principal axes of ellipse B_e lie on the x and y -axis respectively. Let G_e be the Green's function of ellipse B_e . Then, by Lemma 1 and Lemma 3,

$$\int_D G(z_o, z) dx dy \leq \int_{B_e} G(z_o, z) dx dy \leq \frac{\beta^2 - 4y_o^2}{8} \leq \frac{\beta^2}{8}.$$

Using the error bound (5),

$$err(z_o) \leq M \int_D G(z_o, z) dz \leq \frac{M}{8}\beta^2.$$

This is the point-wise intensity error bound for any $z_o \in D$. \square

Theorem 2 says if D is covered by an ellipse, the error is bounded by the term which is proportional to the square of the minor diameter β of the ellipse. The error bound (7) is tighter than the original error bound (6), especially when $\alpha \gg \beta$. Thus, the narrower the inpainting domain, the smaller the error bound (7) will be.

2.3 Minimum of the minor diameter β

In the previous subsection, we showed that when D is covered by an ellipse, the error is bounded by a term proportional to the square of the minor diameter β of the ellipse. From this results, we would like to further refine the error bound if possible. In this section, we consider a local width from $z \in D$ and attempt to refine the result (7). We consider ellipse-like domains with varying width: the domain D is simply connected straight, yet, the thickness varies, as in Fig. 3. We first define local width from a point $z \in D$.

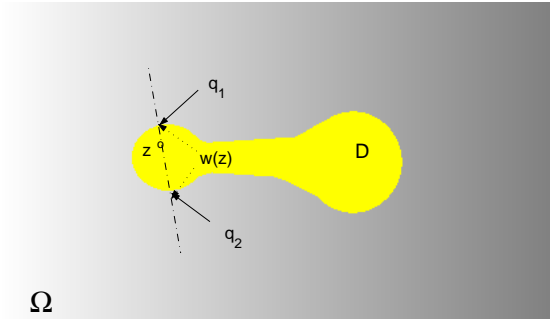


Figure 3: Definition of local width $w(z)$ for point $z \in D$.

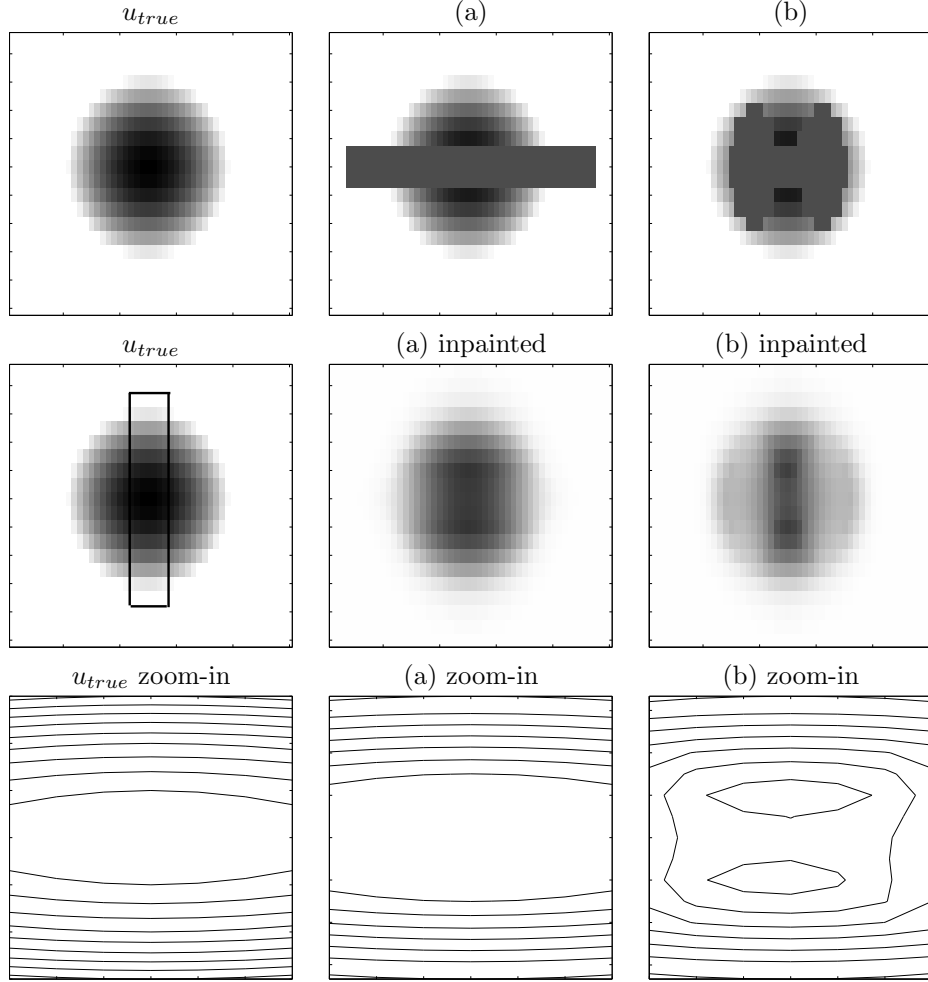


Figure 4: (a) u_o with a line-shaped inpainting domain D_1 , (b) u_o with a dumbbell-shaped inpainting domain D_2 . The total areas of D_1 and D_2 are the same. The third row shows the contour plots of zoom-in of the box in the second row u_{true} . (a) inpainted result is closer to u_{true} .

Definition 1 For a point $z \in D$, consider a straight line l passing through z with at least two intersections with ∂D on the opposite sides from z . Define those two closest intersections to be q_1 and q_2 respectively (Fig. 3). Then define the minimum distance among all such pairs, q_1 and q_2 , to be the local width $w(z)$,

$$w(z) = \min_{\forall l} \|q_1 - q_2\|.$$

In this definition, q_1 and q_2 may not be unique; however, the width w is uniquely defined throughout the region D . With this local width definition, it is tempting to claim that the point-wise inpainting error, $err(z)$, is locally dependent on this local width $w(z)$. However, this is not true, as illustrated in Fig. 4. Inpainting domains of image (a) and (b) have the same local width $w(z)$ and the shape around the center, as well as the same total area. Nevertheless, the inpainted results around the center are quite different, and the error depends on the global shape of the inpainting domain.

Theorem 3 Let β_D be defined by the minimum of β for ellipses covering D ,

$$\beta_D = \inf\{\beta \mid \forall \text{ellipse } B_e(\alpha/2, \beta/2) \text{ covers } D, \text{ i.e. } D \subset B_e\}.$$

Then, for $\forall z \in D$, the point-wise intensity error is bounded by

$$\text{err}(z) \leq \frac{M}{8} \beta_D^2, \quad (8)$$

where M is the smoothness bound for u , $|\Delta u| \leq M$.

Proof. Consider an ellipse B with minor diameter β_D and covers the domain D , s.t. $D \subseteq B$. Let α be the major diameter of the ellipse B . Then, even as $\alpha \rightarrow \infty$,

$$\int_B G(z_o, z) dx dy = \frac{\frac{\beta_D^2}{8} - \frac{\beta_D^2}{\alpha^2} x^2 - y^2}{2 \frac{\beta_D^2}{\alpha^2} + 2} \leq \frac{1}{8} \beta_D^2.$$

Therefore, $\forall z \in D$, the error is bounded by $\frac{M}{8} \beta_D^2$. \square

For images with a straight inpainting domain with varying width, the error is bounded by a term proportional to the square of β_D , which is the lower bound among all possible β :

$$\max_{z \in D} w \leq \beta_D \leq \beta.$$

In this subsection, we illustrate that the error bound is not entirely local, i.e. it can not be locally bounded by a term proportional to the local width w , but the error bound depends on the β_D which is defined from covering the whole inpainting domain by an ellipse. Therefore, the error bound depends on the global shape of the inpainting domain D .

2.4 Torus shaped inpainting domains

In this subsection, we consider the case when the domain D is a torus shape and further refine the error bound from (6) or (7).

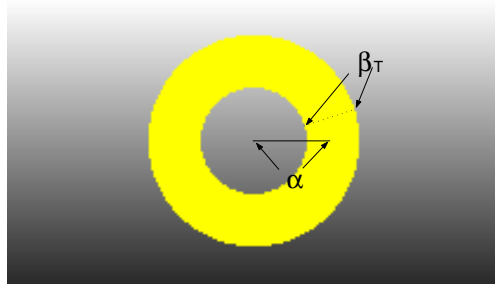


Figure 5: Torus shaped inpainting domain.

Theorem 4 Let a point z be in a torus shaped inpainting domain D , which is defined to be $\alpha - \frac{\beta_T}{2} \leq \|z - z_C\| \leq \alpha + \frac{\beta_T}{2}$, where $\alpha > \frac{\beta_T}{2}$, z_C is the center of the torus. Then for $z_1 = (x_1, y_1) \in D$, the point-wise intensity error, $\text{err}(z_1) = |u(z_1) - u_{\text{true}}(z_1)|$, is bounded by

$$\text{err}(z_1) \leq \frac{M}{4} \left(1 + \frac{1}{\alpha - \frac{\beta_T}{2}}\right) \beta_T^2, \quad (9)$$

where M is a bound for the smoothness of u , $|\Delta u(z)| \leq M$.

Proof. Following the proof of Lemma 3, we consider the Poisson equation on the torus D , and let the unique solution be $v(z)$. For convenience, we assume the center is at the origin $z_C = (0, 0)$. Since torus is

radially symmetric, let's consider the point z on the y -axis, i.e. $z = (0, y) \in D$. Then, v_{yy} is the curvature of the circle at z which is $\frac{1}{r}$ with r as a radius from the center. From $-\Delta v = -(v_{xx} + v_{yy}) = 1$, $v_{xx} = -1 - \frac{1}{r}$ (which is bounded by $-1 - \frac{1}{\alpha - \frac{\beta_T}{2}}$). Since, v_{xx} is bounded and v have zeros at $y = \alpha \pm \frac{\beta_T}{2}$, using polynomial interpolation, $v(y)$ becomes $(-1 - \frac{1}{\alpha - \frac{\beta_T}{2}})(y - (\alpha - \beta_T/2))(y - (\alpha + \beta_T/2))$ for every point on the y -axis. Therefore, $v(z)$ is bounded by the maximum $(1 + \frac{1}{\alpha - \frac{\beta_T}{2}})(\frac{\beta_T}{2})^2$. By similar argument as in Lemma 3, the Green's function of the torus is also bounded by the same term, and using the error form in (5), the bound is calculated. \square

This theorem allows us to further refine the error bound when D can be covered by a torus. The error is bounded by the term proportional to the square of β_T^2 which is the width of the torus. This error bound is smaller than the error bound estimated by either covering by a disk(6) or an ellipse (7). Therefore, one can further refine the error bound when there are additional information available inside the inpainting domain.

2.5 Transformation of a domain

For any inpainting domain, if one covers the domain by an ellipse the error bound is given by (8). However, if we consider the domain when the thickness is small but have complicated shape as in Fig. 6 (a), the error bound given by (8) could be also pessimistic. Considering an ellipse covering D , β_D in (8) is large compared to the local with w . Therefore, in this subsection, we consider a domain transformation to reduce the error bound which is proportional to a new β which is closer to local width w .

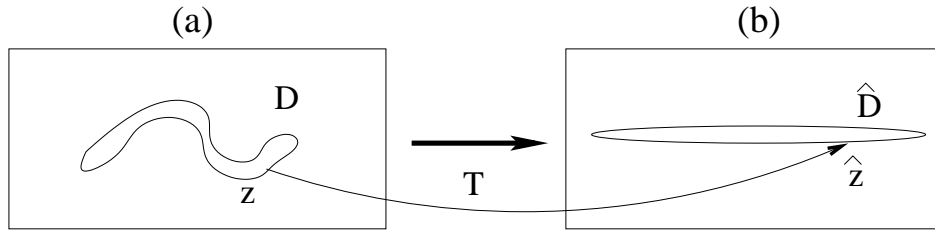


Figure 6: (a) narrow inpainting domain D , (b) transformed domain $\hat{D} = T(D)$.

From the given domain D with smooth boundary that $\partial D \in C^1$, let's define a *skeleton* of the domain to be s . The skeleton of a domain is a way to represent a plane region with a simple graph; for each point $z \in D$, find its closest neighbor in ∂D . If there are more than one such neighbor, it is said to belong to the skeleton of D [20, 22]. Suppose the skeleton of the inpainting domain D is defined by single open curve s which is also C^1 (no branches and smooth).

Let \mathcal{U} be a 2-dimensional manifold, and let P be a projection such that the skeleton s in D becomes a geodesic curve in \mathcal{U} ,

$$P : \Omega \rightarrow \mathcal{U} \text{ and } P(s) = \text{geodesic in } \mathcal{U}$$

Let $\mathcal{G} : \mathcal{U} \rightarrow \mathcal{R}^2$ be a geodesic mapping which maps \mathcal{U} to a Cartesian grid $\mathcal{V} = \mathcal{R}^2$, i.e. this \mathcal{G} maps $P(s)$ into a straight line in \mathcal{V} . Then, define a transformation T to be a domain transformation

$$T = \mathcal{G} \circ P : \Omega \rightarrow \mathcal{V} \tag{10}$$

i.e. this transformation T maps every point on $s \in D \subset \Omega$ onto a geodesic in \mathcal{U} , then maps it onto a straight line in \mathcal{V} . Using this transformation, domain D is mapped to an ellipse-like domain \hat{D} with varying width $\hat{D} = T(D) \in \mathcal{V}$ as in Fig. 6 (b).

Definition 2 We define the skeleton s to be deformable, if the mapping P and \mathcal{G} exists and both are isometry (therefore, T is also isometry).

We are using the standard definition of isometry that a isometry f from M to N is a one-to-one, onto, differentiable function $f : M \rightarrow N$ such that for any curve $\rho : [c, d] \rightarrow M$, the length of ρ equals the length of $f \cdot \rho$ [29]. This transformation T changes the domain Ω to $\hat{\Omega} \subset \mathcal{V}$, and the new image $\hat{u}(z) : \hat{\Omega} \rightarrow \mathcal{R}$ is defined to be $\hat{u}(\hat{z}) = u(T^{-1}(\hat{z}))$ for $\forall \hat{z} = T(z) \in \hat{\Omega}$. In the transformed domain \hat{D} , the inpainting error comes from solving of the new Poisson equation,

$$\begin{cases} -\Delta \hat{u} = \hat{f}, & \forall z \in \hat{D} \\ \hat{u} = 0, & \forall \hat{z} \in \partial \hat{D}, \end{cases}$$

where \hat{f} results from the domain transformation T . Let \hat{M} be the bound for the smoothness, $|\Delta \hat{u}| \leq \hat{M}$. Notice that this smoothness bound \hat{M} may not be the same as M . Since T is isometry (i.e. it is differentiable), \hat{M} is bounded; however, $M \leq \hat{M}$.

Theorem 5 *Let D be the inpainting domain with deformable skeleton s (and associated transformation T). Then, the error bound for $z \in D$ is bounded by*

$$err(z) \leq \frac{\hat{M}}{8} \beta_{\hat{D}}^2,$$

where \hat{M} is the bound for the smoothness $|\Delta \hat{u}| \leq \hat{M}$ and $\beta_{\hat{D}}$ is the minimum of minor diameters of ellipses covering $\hat{D} = T(D)$.

Proof. From equation (8), for $\forall \hat{z} \in \hat{D}$, the error is

$$err(\hat{z}) = |\hat{u}(\hat{z}) - \hat{u}_{true}(\hat{z})| \leq \frac{\hat{M}}{8} \beta_{\hat{D}}^2$$

where, $\beta_{\hat{D}}$ is the minimum of the minor diameter of ellipses covering \hat{D} . Then, the point-wise intensity error term for $\forall z \in D$ is

$$err(z) = |u(z) - u_{true}(z)| = |\hat{u}(T(z)) - \hat{u}_{true}(T(z))|,$$

where $T(z) = \hat{z} \in \hat{D}$ which is also bounded by $\frac{\hat{M}}{8} \beta_{\hat{D}}^2$. \square

Lemma 4 *Let D be the inpainting domain with deformable skeleton s . Then for $\hat{z} \in \hat{D}$, the local width $w(\hat{z})$ at point \hat{z} is bounded by*

$$w(\hat{z}) \leq w(z)$$

where $\hat{z} = T(z) \in \hat{D} = T(D)$ and $z \in D$.

Proof. From definition of local width $w(z)$ at a point z , let l_s be the line segment defining $w(z)$, i.e l_s is part of $l = \arg \min \|q_1 - q_2\|$, between q_1 and q_2 inside D . By definition of deformable skeleton s , the transformation T is isometry. Therefore, the length of $T(l_s)$ is still $w(z)$. However, $T(l_s)$ is no longer a geodesic in \mathcal{V} , therefore, there exists a straight line \hat{l} in \mathcal{V} which defines the new local width $w(\hat{z})$, and this $w(\hat{z})$ is always less than (or equal to) the length of $T(l_s)$. \square

According to this Lemma 4, $\beta_{\hat{D}}$ in the Theorem 5 is a good bound which is related to the thickness of the original domain D . As a summary, in general for a smooth function with harmonic inpainting, the error $err(z)$ at any point $z \in D$, is bounded by a term proportional to the square of either $\beta_{\hat{D}}$ or β_T . These β s acts as the maximum of the local width by considering the global shape of the domain D . The total inpainting error over D for a smooth function with harmonic inpainting is bounded by

$$\int_D err(z) dz \leq \int_D C \hat{M} \tilde{\beta}^2 dz \leq C |D| \hat{M} \tilde{\beta}^2. \quad (11)$$

for some constant C and $\tilde{\beta}$ either of β_D , $\beta_{\hat{D}}$, or β_T .

3 TV Inpainting for piecewise Constant Images

In the previous sections, we showed the case of smooth functions with harmonic inpainting. However, typical images have discontinuities and jumps, and here we investigate the case for piecewise constant images with TV inpainting.

If we consider an interpolation for an 1-dimensional step function with TV inpainting, the error is bounded by the jump of intensity and the length of the inpainting interval. Therefore, in 2-dimensional case, the error is also bounded by the jump of the function as well as the area of the inpainting domain

$$err(D) \leq (I_{max} - I_{min})|D|, \quad (12)$$

where I_{max} and I_{min} are the maximum and the minimum of the possible intensity values. For a bounded variation (BV) function, it makes more sense to consider the total error over D than the point-wise error as in the previous section. Since the point-wise error strongly depends on the location of the point, and the maximum error bound for each point is always, $err(z) = |u(z) - u_{true}(z)| \leq (I_{max} - I_{min})$.

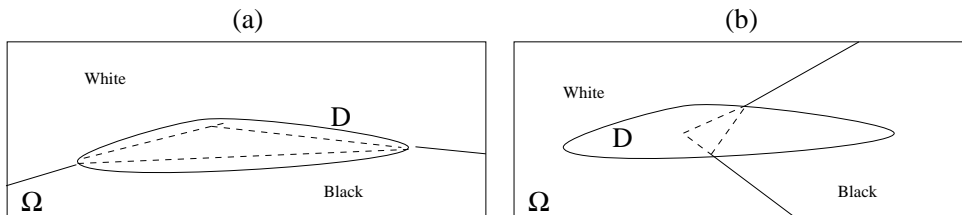


Figure 7: (a) and (b) have the same inpainting domain D ; however, the error regions (the dotted triangles) for two cases are quite different.

Unlike the case for smooth functions, the error is no longer dependent on the β , but on the geometric details of how the level lines meet with the inpainting boundary ∂D . In Fig. 7, the two images (a) and (b) have the same shape and size of D ; however, the possible connections of the level lines are very different, and the connections seem to depend more on the way level lines meet with ∂D . The error becomes the geometrical property of level lines, and being close to the boundary doesn't guarantee smaller error. Identifying the location of the possible error region becomes the focus of error bound for the piecewise constant images. We first define the level line settings and define the error region R which represents the location of the error.

Let Γ_μ be the perimeter of $\{x : u(x) > \mu \text{ s.t. } x \in \Omega \setminus D\}$ which is the level line of image u . Since we are considering piecewise constant case, there exists a integer, $\exists n$ s.t. $\{\Gamma_\mu\} = \{\Gamma_{\mu_i} \mid \text{for } i = 0, 1, \dots, n\}$. Among these $\{\Gamma_{\mu_i}\}$ pick level lines which meet with the inpainting domain D , and refer to them as $\{\Gamma_k\}$. We define l_i to be a *level segment*, if l_i is a continuous segment of Γ_k and meets with ∂D at a unique point q_i . (If l_i meet with ∂D more than once separate l_i into two or more level segments.) Curvature of l_i is κ_i , s_i arc length parameter on l_i . Since any plane curve can be uniquely defined by its curvature, (by Fundamental Theorem of curves) we include the extension of l_i in the direction of curvature inside D i.e. $\frac{d\kappa_i(s_i)}{ds_i} = 0$ with initial curvature $\kappa_i(q_i)$ at q_i .

Since u_{true} is unknown in general, we make the following two assumptions for the piecewise constant true image, u_{true} . This u_{true} is reduced from the information on ∂D in the given original image u_o .

1. We assume that the level lines Γ_k should be a continuous function inside the missing domain D . We define l_{true} to be the true level line connection inside D .
2. We assume the u_{true} has no objects (covered by D) which cannot be recovered from ∂D information alone. Fig. 8 shows an example, where image (a) have objects which are covered by D in image (b), then we consider image (c) as u_{true} (not image (a) as u_{true}). Thus, u_{true} only depends on the information from ∂D .

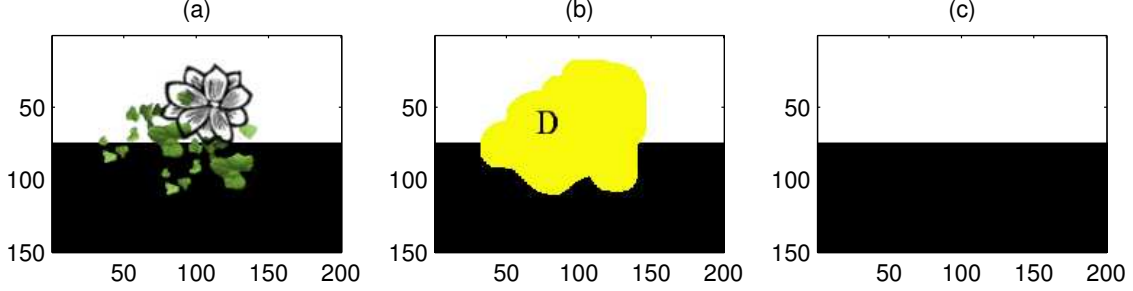


Figure 8: (a) original image, (b) given image u_o with D , (c) u_{true} for image (b).

When TV inpainting method is used, it always connect the level lines with the shortest distance inside D . From the coarea formula for bounded variation functions [18],

$$\int_{R^N} |\nabla u| dx dy = \int_{-\infty}^{\infty} \text{Per}(\{x : u(x) > \mu\}) d\mu,$$

the integral of total variation is minimized when the perimeter $\text{Per}(\{x : u(x) > \mu\})$ is minimized. This occurs when the set $\{x : u(x) > \mu\}$ connects the level lines with the shortest connection. Therefore, when TV inpainting is used, the level lines are connected with the shortest distance inside D in order to minimize the total variation. Let the *shortest connection* between q_i and q_j to be l_{tv} which is defined by using the TV inpainting method. Let the length of l_{tv} be d_{tv} .

In the following section, we consider the geometrical properties of the level lines to better represent the error bound (12), especially using the length d_{tv} .

3.1 Uniquely matching two level lines

Among many level segments l_i of Γ_k (for a fixed k), we assume each level segment has a uniquely matching pair given from u_{true} . Therefore, each level segment has a uniquely matching pair. We assume the matching is already identified, and we only consider each pair separately. Since each time we consider each matching pairs separately, it is similar to considering u as a binary image with only two intensity level and only two level segments are meeting with ∂D . This can be extended to many matching pairs of level lines by considering each pairs one by one.

Definition 3 We define the region surrounded by l_{true} and l_{tv} to be the error region R . $R \subset D$.

The total error of piecewise constant images becomes

$$\text{err}(D) \leq \sum_i \partial I_i |R_i|, \quad (13)$$

where R_i are the each error region from each matching level lines, and $\partial I_i = I_{\max \partial I_i} - I_{\min \partial I_i}$ is the intensity difference across the level segment l_i . This intensity difference ∂I_i is taking values only across from I_i , unlike I_{max} and I_{min} as in (12). This is possible from the second assumption of u_{true} that piecewise constant u_{true} only depends on the boundary ∂D information, and the fact that TV inpainting have a maximum principle.

Theorem 6 If l_{true} is a smooth function $\in C^2$, then the area of the error region is bounded by

$$\text{err}(D) \leq \partial I_{true} \mathcal{M} d_{tv}^3 \quad (14)$$

where $\mathcal{M} = \frac{l_{true}^{(2)}(\zeta)}{12}$ is the bound for the smoothness of l_{true} with respect to l_{tv} , and ∂I_{true} the intensity difference across l_{true} .

Proof. The difference between l_{tv} and l_{true} can be calculated by a linear polynomial approximation. Let q_1 and q_2 be the two points where l_{true} and l_{TV} meets at the boundary ∂D , then $l_{true} \in C^2$ and l_{tv} linearly interpolates l_{true} at two points q_1 and q_2 . Let \vec{x} be in the direction of l_{tv} and \vec{y} be in the direction perpendicular to \vec{x} , then for the arc length x defined on l_{tv} , the distance between two curves l_{tv} and l_{true} is bounded by

$$\int_{q_1}^{q_2} \frac{1}{2} l_{true}^{(2)}(\zeta)(x - q_1)(x - q_2) \leq \mathcal{M} \frac{d_{tv}^3}{12},$$

where the derivative is with respect to x i.e. $\frac{\partial^2 l_{true}}{\partial x^2}$. \square

This Theorem 6 covers the most common case of the level line connection which is the two matching level lines are a part of one smooth curve. The smaller the distance d_{tv} is the smaller the total error will be by a cube power. The distance d_{tv} is a strong factor for the area of the error region $|R|$.

If $l_{true} \notin C^2$ i.e. it is continuous but not a smooth curve, then we use the following Lemmas to show that the area of R is bounded by a term proportional to d_{tv}^2 . For particular cases, we can express the area of this error region $|R|$ using the d_{tv} , κ_i and the direction of the level segments. If l_{true} is C^1 , we assume l_{true} has only one discontinuous point \hat{q} inside D , and l_{true} is defined by two level segments l_1 and l_2 . The direction θ_i is defined to be the angle between l_{tv} and a line connecting \hat{q} and q_i , the angle is taken inside the domain D .

Lemma 5 *When the level segments, l_1 and l_2 , meeting with ∂D are straight lines and have a unique intersection \hat{q} inside D , i.e. $\kappa_1 = \kappa_2 = 0$, $\theta_1 \cdot \theta_2 > 0$ and $|\theta_1 + \theta_2| < \pi$, then*

$$|R| \leq \mathcal{O}(d_{12}^2 \theta).$$

The area $|R|$ is a function of d_{tv} , θ_1 and θ_2 where $\theta = \max\{\theta_i \text{ for } \theta_i < \pi/2, i = 1, 2\}$.

Proof. Let l_h be a line perpendicular to l_{tv} that passes through the intersection \hat{q} . Let b_1 be the distance between q_1 and l_h along l_{tv} ($d_{tv} = b_1 + b_2$ if l_h is between q_1 and q_2 , and $d_{tv} = |b_1 - b_2|$ otherwise). Then the area of triangle is

$$|R| = \frac{1}{2}(b_1^2 g(\tan \theta_1) + b_2^2 g(\tan \theta_2)),$$

where $g(x) = x$, and $g(x) = 0$ only if $x = \infty$. By definition, function g ignores the case when $\theta_i = \frac{\pi}{2}$. (If $\theta_1 = \frac{\pi}{2}$, it is a right triangle with area $\frac{1}{2} b_1^2 \tan \theta_2$.) This equation holds as long as all $\theta_i > 0$ and $\theta_1 + \theta_2 < \pi$. Let $\theta = \max\{\theta_i \text{ for } \theta_i < \pi/2, i = 1, 2\}$, then the error is bounded by $\frac{1}{2} d_{tv}^2 \tan \theta \approx \mathcal{O}(d_{tv}^2 \theta)$. \square

Lemma 5 considers the case when there is a corner inside D and the error region R is a triangle surrounded by l_1 , l_2 and l_{tv} , the area of the error region is bounded by the term proportional to the square of d_{tv} and the angle θ . The following Lemma covers the more general case, when the level lines have different curvatures and have one intersection inside D .

Lemma 6 *When two, curved or straight, level lines l_1 and l_2 have one intersection \hat{q} inside D , i.e. $\kappa_1 \neq \kappa_2$, and $\theta_1 \cdot \theta_2 > 0$ and $|\theta_1 + \theta_2| < \pi$, then*

$$|R| \leq \mathcal{O}(d_{tv}^2 h(d_{tv}, \mathcal{M}, \theta)).$$

Here $\theta = \max\{\theta_i \text{ for } \theta_i < \pi/2, i = 1, 2\}$, and \mathcal{M} is the maximum bound for the smoothness of l_1 and l_2 with respect to the line connecting \hat{q} and q_i .

Proof. As in Lemma 5, the area of a triangle defined by the three points q_1 , q_2 and \hat{q} , is $\frac{1}{2}(b_1^2 s(\tan \theta_1) + b_2^2 s(\tan \theta_2))$. Let's refer to this triangle-region as A , then depending on the sign of the curvature κ_i , the error region R is either bigger or smaller than triangle A . For example, if $\kappa_2 < 0$, the area $|R|$ is bigger than that of $|A|$, and if $\kappa_i > 0$, then $|R|$ is smaller than $|A|$. The amount of the difference between $|R|$ and $|A|$

can be calculated using equation (14). Then the distance between q_i and \hat{q} is $\frac{b_i}{\cos \theta_i}$. Therefore, the area of the error region $|R|$ becomes,

$$|R| = \sum_{i=1,2} \left\{ \frac{1}{2} b_i^2 s(\tan \theta_i) \pm \mathcal{M}_i \left(\frac{b_i}{\cos \theta_i} \right)^3 \right\} \leq \mathcal{O}(d_{tv}^2 (\theta + \mathcal{M} \frac{d_{tv}}{\cos^3 \theta}))$$

where $h(d_{tv}, \mathcal{M}, \theta) = \theta + \mathcal{M} \frac{d_{tv}}{\cos^3 \theta}$, \mathcal{M}_i is the bound for the smoothness of l_{true} with respect to the straight line connecting q_i and \hat{q} , i.e. $|\frac{\partial^2 l_{true}}{\partial s^2}| \leq \mathcal{M}_i$ where s is a arc parameter on the line connecting q_i and \hat{q} . \mathcal{M} is the maximum among \mathcal{M}_i . \square

Theorem 7 When $l_{true} \in C^n$ with $n \geq 2$, or $l_{true} \in C^1$ and has a unique discontinuous point inside D , the area of the error region $|R|$ is bounded by a term proportional to d_{tv}^2 , and the total error is bounded by

$$err(D) \leq \partial I \mathcal{O}(d_{tv}^2 f(d_{tv}, \mathcal{M}, \theta)),$$

where \mathcal{M} , θ and f are defined from above Lemmas.

For smooth functions with harmonic inpainting, the error was bounded by a term proportional to $\tilde{\beta}^2$, and for the piecewise constant images with TV inpainting, the error is bounded by a term proportional to d_{tv}^2 . The shorter the distance d_{tv} is, the smaller the error region will be.

3.2 Multiple possible connections of level lines and higher order inpainting methods

In this section, we briefly consider the case with multiple possible connections. These are cases when the level lines are paired but the possible connections are not unique. For example, as in Fig. 9 (a), there are two possible connections among the level lines meeting with ∂D which are l_c and l_f . Define l_c to be *the shortest possible connection* and l_f to be *level line extension following the curvature direction*. TV inpainting always prefers the shortest connection l_c to minimize $\text{Per}(\{x : u(x) > \mu_i\})$, as the inpainted result is shown in Fig. 9 (b), i.e. $l_c = l_{tv}$. To account for other possible connections such as l_f , the error region R_m for this multiple possible connection case should be the polygon defined by connecting all the intersections q_i :

$$|R_m| = \text{the polygon determined by connecting all } q_i.$$

In Fig. 9, TV inpainting connects l_c , and the error region is the rectangle with l_c and l_f as the two sides. In general, unless the inpainting domain is narrow and l_c agrees with the true image connection in u_{true} , TV inpainting results in a big error region.

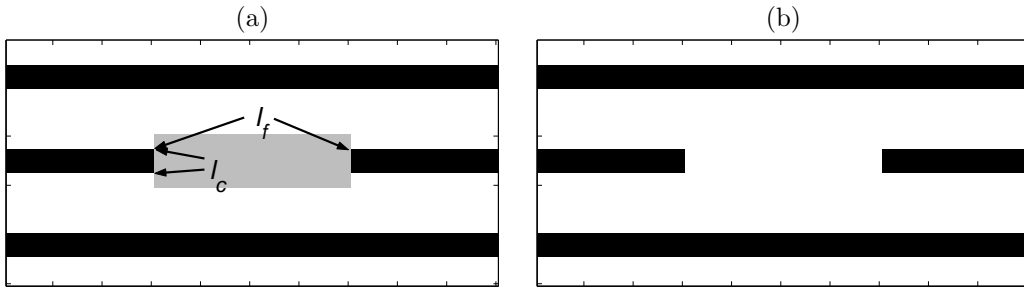


Figure 9: (a) the gray box in the center is D . The level lines have two different possible connections: l_c and l_f . (b) TV inpainting result. TV inpainting prefers l_c .

For these cases with multiple possible connections, when higher order inpainting method is used, the error region can be further reduced. Here, we consider the Euler's Elastica method [9]

$$\min \int_{\Omega} |\nabla u|(a + b\kappa^2) dx dy + \frac{\lambda}{2} \int_{\Omega \setminus D} |u - u_o|^2 dx dy \quad (15)$$

to illustrate such results. We use reasonable guesses for the two parameters a and b . For a piecewise constant image u , using the coarea formula for the Elastica model, it becomes

$$\int_D |\nabla u|(a + b\kappa^2) dx dy \sim \int_{-\infty}^{\infty} \left[\int_{\{u=\mu\}} a + b\kappa^2(s) ds \right] d\mu,$$

where s is a arc length along the perimeter of $\{x : u(x) = \mu\}$. As an inpainting result, the two terms should be minimized: the perimeter $\int_{\{u=\mu\}} 1 ds$ and the curvature $\int \kappa^2(s) ds$ of the level lines. Thus, the length of the connection should be relatively short, while smoothly connecting the two level lines without any kinks or sharp corners. Let l_{curv} be such a curve connecting two matching level lines, connecting intersections q_1 and q_2 with smoothly changing curvature κ , i.e.

$$\min \frac{d\kappa(s)}{ds}, \quad s \in D \text{ and } \kappa(q_i) = \kappa_i, \text{ for } s \in \partial D.$$

Then the error region for using this Elastica model becomes,

$$|C| = \text{the area surrounded by } l_{true} \text{ and } l_{curv}. \quad (16)$$

The difference between TV inpainting (3) and Elastica model (16) is having l_{curv} instead of l_{tv} (the straight line connecting q_1 and q_2). This l_{curv} is closer to the true image u_{true} , since it incorporates the curvature information. In general the error region from Elastica model is smaller than that from TV inpainting, $|C| \ll |R|$. Moreover, for the case with multiple possible connections (as in Fig. 9), Elastica model connects l_f with l_{curv} , and the inpainting result will be closer to the true image l_{true} . Therefore, when higher order inpainting methods are used, the error region can be further reduced by the l_{curv} connection.

4 TV Inpainting for Bounded Variation Images

In previous sections, we studied the cases for smooth functions with harmonic inpainting, and piecewise constant images with TV inpainting. In this section, we consider a particular type of bounded variation functions with TV inpainting. In [21], authors showed that the total variation of natural image can blow up when resolution of image increases; however, in this section, we consider BV as image space, and consider a particular type of piecewise continuous images.

In section 2, we used harmonic inpainting instead of TV inpainting for continuous image $u \in C^2$, since it is more natural for continuous images. However, for BV function with discontinuity, TV inpainting works better in getting sharp edges. The harmonic inpainting solution u is the solution to

$$\Delta u = 0, \quad (17)$$

while TV inpainting solution u is the solution to

$$\nabla \cdot \left(\frac{\nabla u}{|\nabla u|} \right) = 0 \quad (18)$$

which in practice $|\nabla u_\epsilon| = \sqrt{u_x^2 + u_y^2 + \epsilon}$ is used for $|\nabla u|$ in the denominator to avoid singularities. The difference between harmonic inpainting and TV inpainting is at the diffusion coefficient $\frac{1}{|\nabla u_\epsilon|}$. For a smooth continuous function where exists a bound for a smoothness $|\nabla u| \leq M$, $|\nabla u_\epsilon|$ is bounded by $\epsilon \leq |\nabla u_\epsilon| \leq M + \epsilon$.

Therefore, $\frac{1}{M+\epsilon} \leq \frac{1}{|\nabla u_\epsilon|} \leq \frac{1}{\epsilon}$. Suppose u is a solution to (17), then it is also a solution to equation (18), since the right hand side of equation (18) is bounded by

$$\frac{1}{M+\epsilon} \Delta u \leq \nabla \cdot \left(\frac{\nabla u}{|\nabla u_\epsilon|} \right) \leq \frac{1}{\epsilon} \Delta u, \quad \text{with } \Delta u = 0.$$

In addition, if u is a solution to (18), from above inequality $\Delta u = 0$. Thus, we assume the error bound for using TV inpainting is the same as in harmonic case (8) for smooth continuous regions. In section 5, we also numerically compared using harmonic inpainting and TV inpainting for a smooth function (Fig. 11).

As for the error bound for BV image u , in the BV space typically the norm is defined as $|u|_{BV(\Omega)} = |u|_{L^1(\Omega)} + \int_\Omega |Du|$, where $\int_\Omega |Du|$ is the distributional gradient of u [1]. However, to be consistent with the previous sections, we consider $err(z) = |u(z) - u_{true}(z)|$ as the error in this section.

Theorem 8 *For piecewise continuous functions u^* defined as $u^* = u^s + u^d$, where u^s is a smooth function and u^d is a piecewise constant function, then the error bound for using TV inpainting is*

$$err(D) = \int_D |u(z) - u_{true}(z)| dz \leq \frac{1}{8} |D| \hat{M}(u^s) \tilde{\beta}^2 + \partial I(u^d) \cdot |R(u^d)|$$

where \hat{M} is the smoothness bound for u^s , $\tilde{\beta}$ is determined from the shape of D by either of β_D , $\beta_{\bar{D}}$ or β_T . $\partial I(u^d)$ is the maximum intensity difference of u^d on ∂D , and the error region R is defined from the level lines of u^d .

Proof. The error term for image u^* on D is,

$$err(D) = \int_D |u^*(z) - u_{true}^*(z)| dz \leq \int_D |u^s(z) - u_{true}^s(z)| dz + \int_D |u^d(z) - u_{true}^d(z)| dz$$

by the definition of function $u^* = u^s + u^d$. For smooth function u^s , the error is bounded by the equation (11), and for piecewise constant function u^d , the error is bounded by $\partial I|R|$ as in section 3. Therefore, for piecewise continuous function u^* defined by $u^* = u^s + u^d$, the bound for the total error is the addition of two error bounds. \square

Theorem 8 shows that for a particular type of BV functions, the error bounds from previous sections can be utilized and represents the dependence of $\hat{\beta}$ and d_{tv} .

5 Numerical Experiments

In this section, we present some numerical experiments to validate the theoretical error bound we derived in the previous sections. For the numerical computation, instead of using the constrained minimization problem (1), we use the unconstrained equation such as

$$J_\lambda(u) = \int_\Omega g(u) dx dy + \frac{\lambda}{2} \int_{\Omega \setminus D} |u - u_o|^2 dx dy$$

with the Euler-Lagrange equation. We use simple finite difference schemes as well as the digital TV filter [10] type methods for the computations. For harmonic inpainting, we solve $u_t = \Delta u + \lambda_D(u_o - u)$, with a big value for $\lambda_D(z)$ for $z \in \Omega \setminus D$, and $\lambda_D(z) = 0$ for $z \in D$. For TV inpainting, we use methods described in [11]. As for color image inpainting, we considered color as a RGB color vector and used the vectorial TV inpainting method [8, 24]. (Color images of this paper can be found at [7].)

The first example, Fig. 10, is harmonic inpainting for smooth functions. From section 2, the total error bound was given by $err(D) = \frac{1}{8} M \beta_D^2 |D|$. From image (a) to (c), β_D is increasing by a factor of 1.5, while the areas of the inpainting domains remains the same. The graph (d) is a plot of L^∞ difference between each image and u_{true} , and a quadratic function shows that the error is bounded by a term proportional to

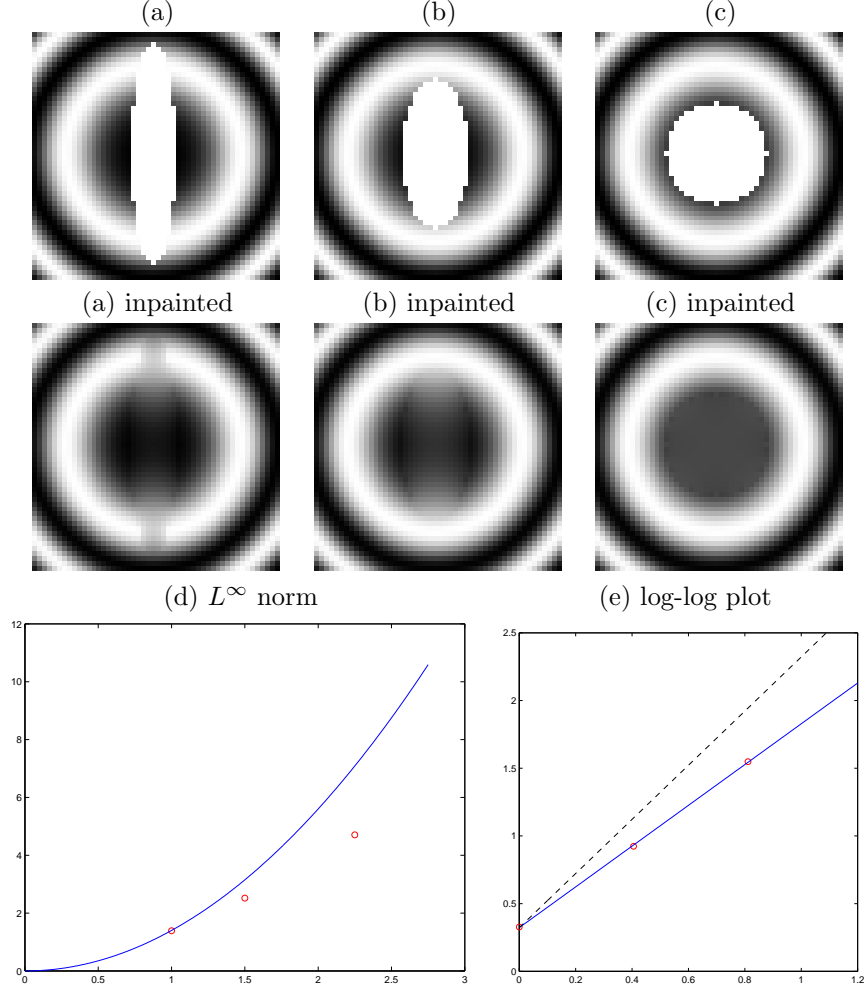


Figure 10: (a), (b), and (c) are u_o with different D (white ellipses and a circle). All inpainting domains have the same total area, while β are increasing by a factor of 1.5. (d) is a plot of L^∞ difference between each inpainted result and u_{true} . The dots are the error and the curve is a quadratic function. (e) is the log-log plot of (d), and the dotted line has a slope 2.

β_D^2 . The graph (e) shows a log-log plot of the errors, i.e. $\log err(D)$ versus $\log \beta_D$, and the slope of the errors are also bounded by the linear function with slope 2 (a dotted line). Numerical result is consistent with the error bound (8).

Fig. 11 is an example of the comparison between harmonic inpainting, TV inpainting, and Euler's Elastica model (15) for a smooth image. In section 4, we assumed the difference between using harmonic inpainting and TV inpainting are negligible, and Fig. 11 shows that the errors are indeed similar. For this experiment, u_{true} as well as the inpainting domains are the same as the numerical example in Fig. 10, and the width β_D is increasing by a factor of 1.5. The graph (a) shows L^∞ difference between each inpainting results and u_{true} , and all the results are similar. The log-log plots of the L^∞ difference in graph (b) also shows that all error are bounded by a linear function with a slope 2.

As in the cases of section 3.1, Fig. 12 is an example of a piecewise constant image using TV inpainting for uniquely matching two level lines. By applying Lemma 5 to calculate $|R|$, for image (a), the area of the error region is $|R| \approx 0$, while for image (b), it is $|R| \approx \frac{d_{tv}^2}{2}$. The error for image (b) is bigger since the angle

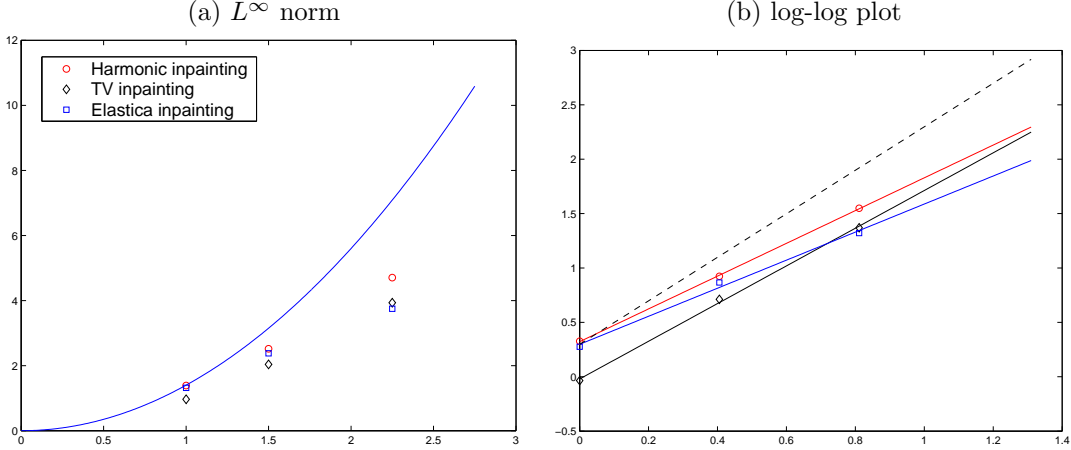


Figure 11: Comparison of harmonic inpainting, TV inpainting, and Euler's Elastica (15) for a smooth function. (Experiments are the same as Fig. 10). The error are bounded by a quadratic function and the slope of log-log plots are bounded by 2.

θ and d_{tv} are bigger in image (b). This is consistent with the numerical result that image (b) have a bigger noticeable error (the corner of number 2 is missing).

Next example is the case in section 3.2, when level lines meeting with ∂D have multiple possible connections. Given l_f and l_c , TV inpainting always prefers the closer connection l_c , and Fig. 13 shows an example of having different l_c . Comparing images (a) and (b), l_c for image (a) is the true connection, while for image (b), l_f is the true connection. Therefore, image (a) gives better results, and TV inpainting always prefers closer connection l_c .

Final couple of results are using TV inpainting for general piecewise continuous images. In Fig. 14 and Fig. 15, the widths of each inpainting domain are increasing by a factor of 2 while keeping the same total area. The inpainting results shows that the narrower the inpainting domain the better the result. Two plots (a) and (b) in Fig. 16 show the L^∞ difference between each inpainting result and u_{true} , for Fig. 14 and Fig. 15 respectively.

6 Conclusion

We have investigated the error bounds for image inpainting problems. For general inpainting experiments, local inpainting methods are known to work well for narrow inpainting domains, and the error analysis in this paper give some analysis on this phenomenon. For a smooth function with harmonic inpainting, the error is bounded by a term proportional to the square of $\tilde{\beta}$,

$$err(D) \leq \frac{1}{8}|D|\hat{M}\tilde{\beta}^2.$$

This $\tilde{\beta}$ is the global maximum of the local width of the inpainting domain which is either β_D , $\beta_{\bar{D}}$ or β_T , and \hat{M} depends on how complicated the shape of D is. For a smooth function, the inpainting error depends on the global shape of the inpainting domain. For a piecewise constant image with TV inpainting, the error is more locally determined by the error region R ,

$$err(D) \leq \partial I|R| \leq \partial I\mathcal{O}(d_{tv}^2 f(d_{tv}, \mathcal{M}, \theta))$$

for some function f defined in section 3. The distance between the level lines d_{tv} is one of the major factor, and the error is bounded by a term proportional to the square of d_{tv} . The width $\tilde{\beta}$ and the distance d_{tv}

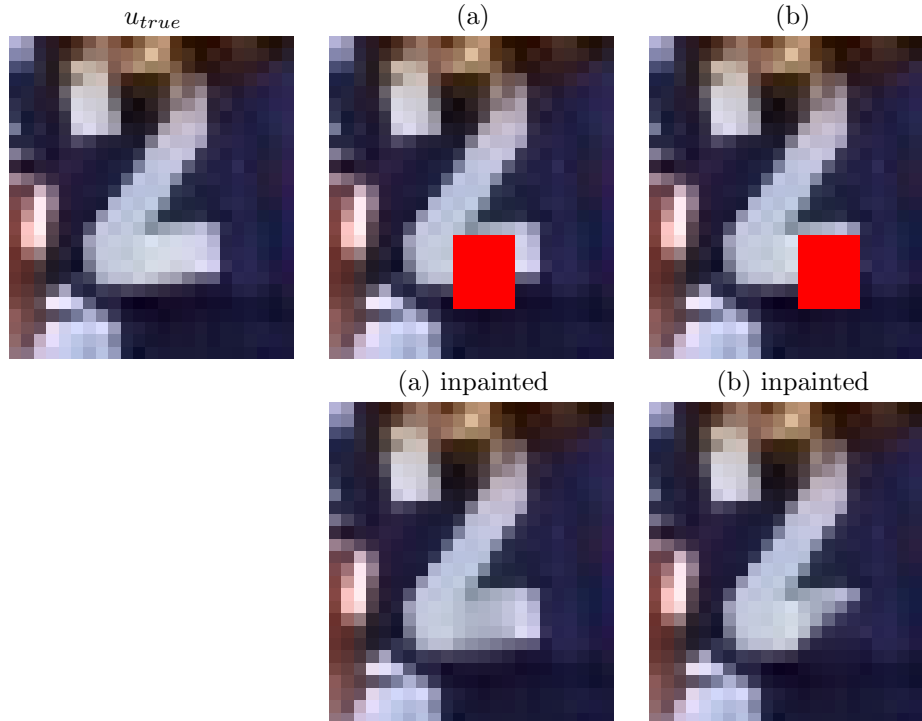


Figure 12: (a) and (b) are different u_o with the same square D in different locations. Image (b) have bigger θ_1 , θ_2 , and d_{tv} , compared to those of image (a). The inpainted results reflect the different error regions. The corner is missing in (b) inpainted.

play important rules in the error bound for image inpainting. Therefore, the narrower $\tilde{\beta}$ and the smaller d_{tv} , the smaller the error bound will be, and the inpainting results will be better when the inpainting domain is narrow.

References

- [1] G. Aubert and P. Kornprobst. *Mathematical Problems in Image Processing: Partial Differential Equations and the Calculus of Variations*, volume 147 of *Applied mathematical sciences*. Springer-Verlag, New York Inc, 2002.
- [2] C. Ballester, M. Bertalmio, V. Caselles, G. Sapiro, and J. Vergera. Filling-in by joint interpolation of vector fields and gray levels. *IEEE Trans. Image Processing*, 10(8):1200–1211, 2001.
- [3] M. Bertalmio, A. Bertozzi, and G. Sapiro. Navier-Stokes, fluid dynamics, and image and video inpainting. *Proc. IEEE Computer Vision and Pattern Recognition(CVPR), Hawaii*, 2001.
- [4] M. Bertalmio, G. Sapiro, V. Caselles, and C. Balleste. Image inpainting. *Proceedings of SIGGRAPH 2000, New Orleans*, 2000.
- [5] M. Bertalmio, Luminita Vese, G. Sapiro, and S. Osher. Simultaneous structure and texture image inpainting. *IEEE Trans. Image Processing*, 12(8):882–889, 2003.
- [6] V. Caselles, J. M. Morel, and C. Sbert. An axiomatic approach to image interpolation. *IEEE Trans. Image Processing*, 7(3):376–386, 1998.

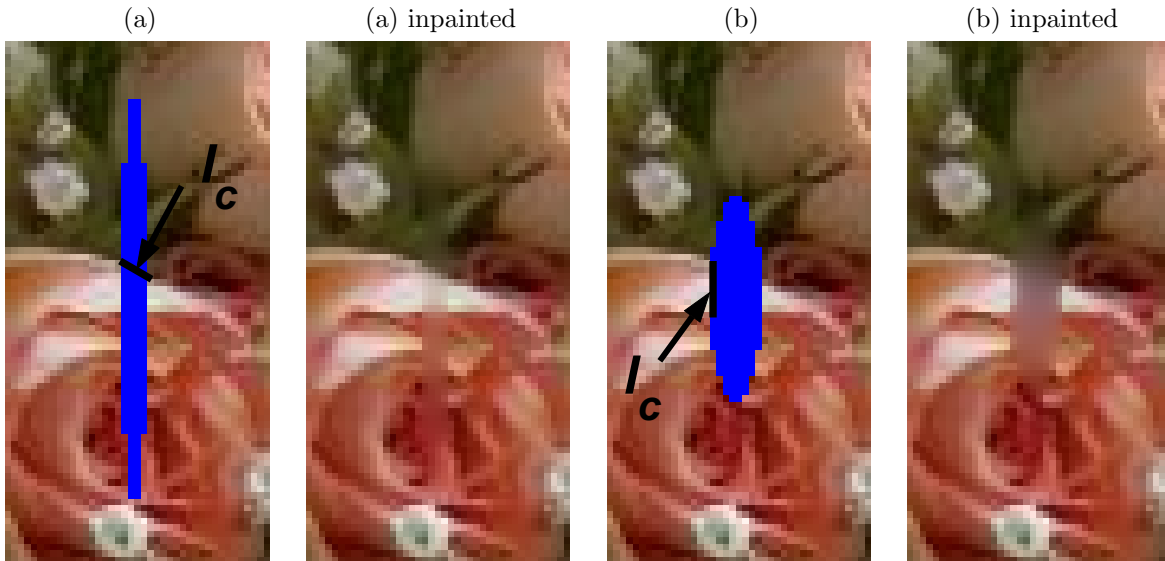


Figure 13: (a) and (b) have two different inpainting domains, and l_c in (a) and (b) are different. TV inpainting prefers the closer connection l_c , as shown in the results.

- [7] T. F. Chan and S. H. Kang. Error analysis for image inpainting. *UCLA CAM 04-72*, 2004.
- [8] T. F. Chan, S. H. Kang, and J. Shen. Total variation denoising and enhancement of color images based on the CB and HSV color models. *Journal of Visual Comm. and Image Rep.*, 12(4):422–435, 2001.
- [9] T. F. Chan, S. H. Kang, and J. Shen. Euler’s elastica and curvature based inpainting. *SIAM Journal of Applied Math.*, 63(2):564–592, 2002.
- [10] T. F. Chan, S. Osher, and J. Shen. The digital TV filter and nonlinear denoising. *IEEE Trans. Image Process.*, 10(2):231–241, 2001.
- [11] T. F. Chan and J. Shen. Mathematical models for local deterministic inpaintings. *SIAM Journal of Applied Math.*, 62(3):1019–1043, 2001.
- [12] T. F. Chan and J. Shen. Morphology invariant PDE inpaintings. *Technical report, UCLA Dept. of Math.*, CAM 01-15, 2001.
- [13] T. F. Chan and J. Shen. Non-Texture inpainting by curvature-driven diffusion (CDD). *Journal of Visual Comm. and Image Rep.*, 12(4):436–449, 2001.
- [14] T. F. Chan and J. Shen. *Image Processing and Analysis: variational, PDE, wavelets, and stochastic methods*. SIAM Publisher, Philadelphia, 2005.
- [15] T. F. Chan, J. Shen, and H. M. Zhou. Total variation wavelet inpainting. *UCLA CAM report*, 04-47, 2004.
- [16] T. F. Chan, L. Vese, and J. Shen. Variational PDE models in image processing. *AMS Notice*, 50:14–26, 2003.
- [17] L. Evans. *Partial Differential Equations*. American Mathematical Society, 1998.
- [18] L. Evans and R. Gariepy. *Measure Theory and Fine Properties of Functions*. Studies in Advanced Mathematics. CRC Press, Boca Raton, FL, 1992.

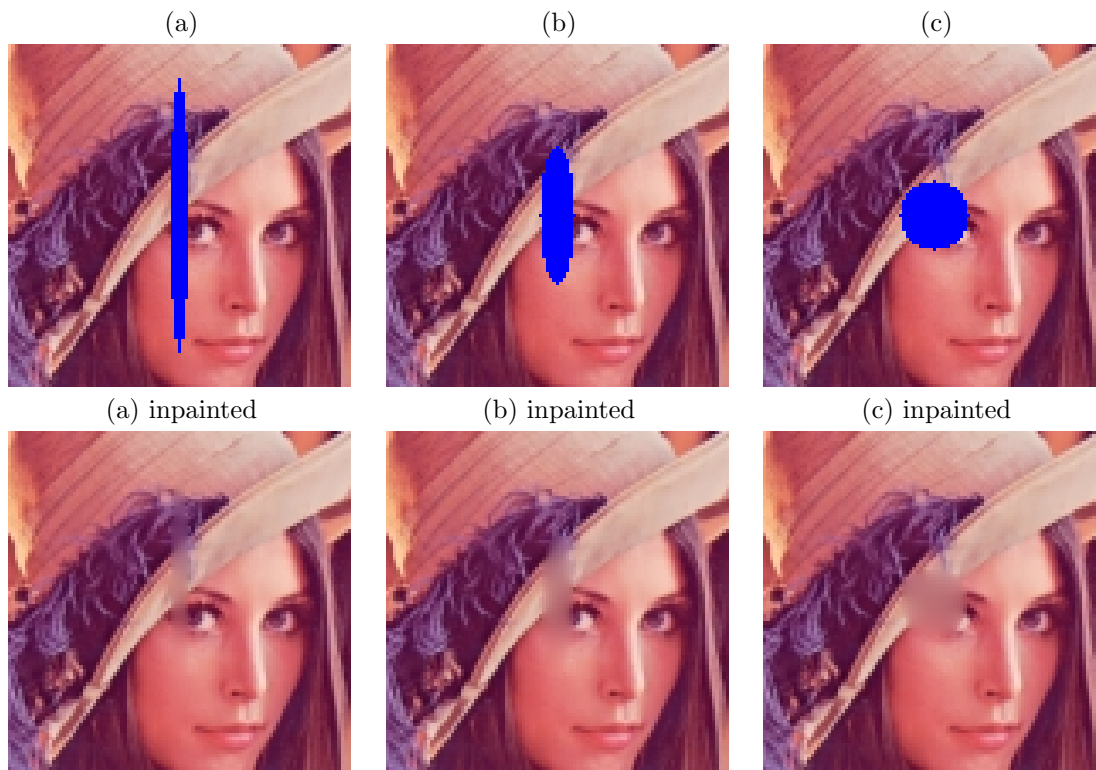


Figure 14: The first row shows the given images u_o with different inpainting domains. The second row is the inpainted results, respectively.

- [19] D. Gilbarg and N.S. Trudinger. *Elliptic Partial Differential Equations of Second Order*. Springer-Verlag, Berlin, 1977.
- [20] R. Gonzalez and P. Woods. *Digital Image Processing*. Addison-Wesley Publishing Company, 1992.
- [21] Y. Gousseau and J.-M. Morel. Are natural images of bounded variation. *SIAM Journal of Mathematical Analysis*, 33(3):634–648, 2001.
- [22] A. Jain. *Fundamentals of Digital Image processing*. Prentice Hall, 1989.
- [23] F. John. *Partial Differential Equations*, volume 1 of *Applied mathematical sciences*. Springer-Verlag, New York Inc, 1981.
- [24] S. H. Kang. Mathematical approaches to color denoising and image inpainting problems. *UCLA CAM 02-25*, 2002. Ph. D Thesis.
- [25] S. H. Kang, T. F. Chan, and S. Soatto. Inpainting from multiple view. *IEEE Proceedings of First International Symposium on 3D Data Processing Visualization Transmission*, pages 622–625, 2002.
- [26] S. H. Kang, T. F. Chan, and S. Soatto. Landmark based inpainting from multiple view. *UCLA CAM report*, 02-11, 2002.
- [27] S. Masnou. Variational formulation of the disocclusion problem. *The abdu salam, int'l centre for theoretical physics, school on mathematical problems in image processing*, 2000.
- [28] S. Masnou and J. M. Morel. Level lines based disocclusion. *Proceedings of 5th IEEE Int'l Conf. on Image Process., Chicago*, 3:259–263, 1998.

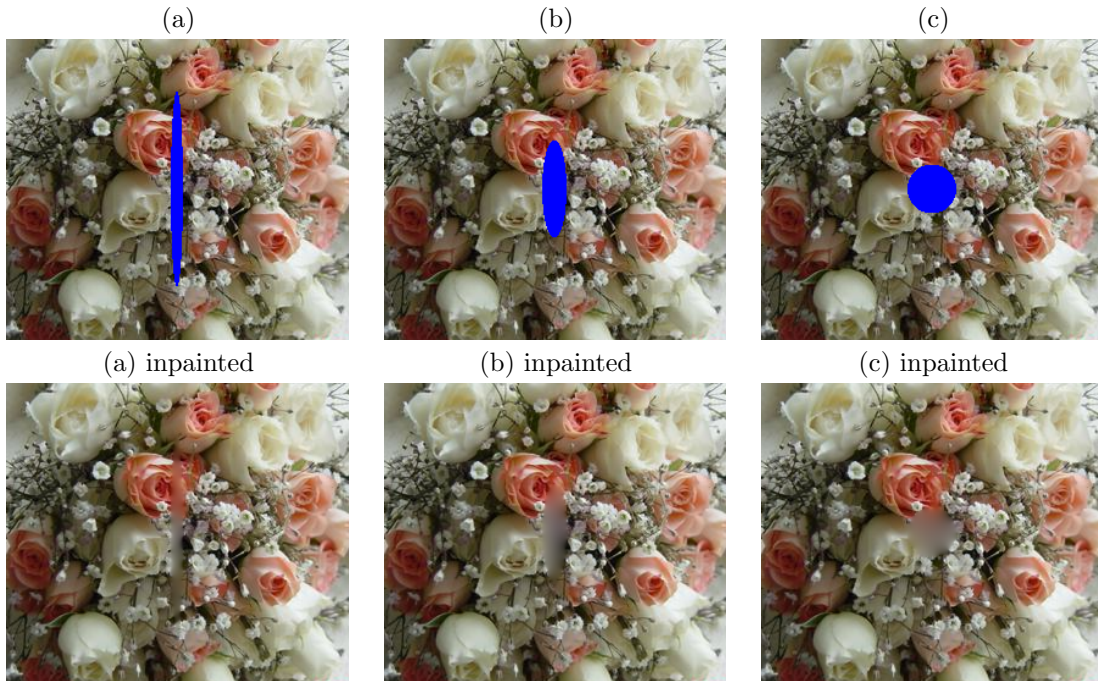


Figure 15: The first row shows the given images u_o with different inpainting domains. The second row is the inpainted results, respectively.

[29] R. Millman and G. Parker. *Elements of Differential Geometry*. Prentice Hall, 1977.

[30] I. Peterson. Filling in blanks. *Science news*, 161(19), May 11,2002.

[31] G. Sapiro. Image inpainting. *SIAM News*, 35(4), May, 2002.

[32] J. Shen. Inpainting and the fundamental problem of image processing. *SIAM News*, 36(5), 2003.

[33] J. Shen and S. Esedoglu. Digital inpainting based on the mumford-shah-euler image model. *Europ. J. Appl. Math.*, 13:353–370, 2002.

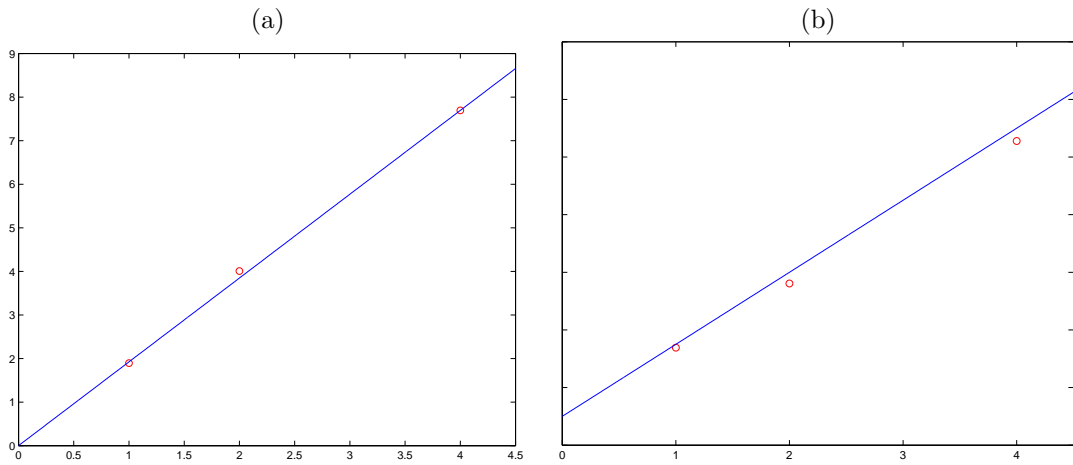


Figure 16: (a) L^∞ difference between u_{true} and TV inpainting results of Fig. 14. (b) L^∞ difference of Fig. 15. As the width β increases, the error strictly increases.